HHS Public Access

Author manuscript

Int J Radiat Oncol Biol Phys. Author manuscript; available in PMC 2023 January 01.

Published in final edited form as:

Int J Radiat Oncol Biol Phys. 2022 January 01; 112(1): 222–236. doi:10.1016/j.ijrobp.2021.08.015.

Mechanisms and review of clinical evidence for variations in relative biological effectiveness in proton therapy

Harald Paganetti, PhD

Department of Radiation Oncology, Massachusetts General Hospital & Harvard Medical School, Boston, Massachusetts, USA

Abstract

Proton therapy is increasingly being used as a radiation therapy modality. There is uncertainty about the biological effectiveness of protons relative to photon therapies as it depends on several physical and biological parameters. Radiation oncology currently applies a constant and generic value for the relative biological effectiveness (RBE) of 1.1, which was chosen conservatively to ensure tumor coverage. The use of a constant value has been challenged particularly when considering normal tissue constraints. Potential variations in RBE have been assessed in several published reviews but have mostly focused on data from clonogenic cell survival experiments with unclear relevance for clinical proton therapy. The goal of this review is to put in vitro findings in relation to clinical observations. Relevant in vivo pathways determining RBE for tumors and normal tissues are outlined, including not only damage to tumor cells and parenchyma but also vascular damage and immune response. Furthermore, the current clinical evidence of varying RBE is reviewed. The assessment can serve as guidance for treatment planning, personalized dose prescriptions, and outcome analysis.

Introduction

Radiation therapy treatment planning is based on prescription doses and normal tissue constraints that are defined empirically and site specific. When treating patients with protons, the potential difference in biological effect compared to photons for the same dose is considered by applying a relative biological effectiveness (RBE), defined as the ratio of photon versus proton dose to reach the same level of effect. In treatment planning for proton therapy (PT), all treatments are currently prescribed using an RBE of 1.1. This value was agreed upon in the early days of PT as a conservative average for tumor control. The use of

Corresponding author: Harald Paganetti, Massachusetts General Hospital, Department of Radiation Oncology, 100 Blossom Street, Cox-3 Room 350, Boston, MA 02114, Phone +1 617 726 5847, hpaganetti@mgh.harvard.edu.

Conflict of Interest Statement

The author declares that there is no conflict of interest. The sole author was responsible for literature review, analysis and interpretation of data and drafting of the manuscript. He takes full responsibility for the integrity of the data and accuracy of the data analysis.

Data Availability Statement for this Work

Research data are stored in an institutional repository and will be shared upon request to the corresponding author.

a generic, spatially invariant RBE within tumor and normal tissue structures disregards the evidence that the RBE varies with LET (linear energy transfer), physiological and biological factors, and clinical endpoint.

A mathematical expression for the RBE based on the linear-quadratic dose-response relationship is shown in equation (1) [1]. Accordingly, the proton RBE is a function of α_x and β_x of the reference photon radiation, α and β of the proton radiation (depending on the proton LET), and the proton dose per fraction, D_p (neglecting dose rate and time-dependent repair corrections). In this article, LET is reported as dose-averaged LET_d in units of keV/μm [2]. Several empirical RBE models have been developed based on fits to clonogenic cell survival (CCS) data from various cell lines. A comparison of these models showed consistent trends but revealed considerable variations in absolute RBE values [3]. One of these models is shown in equation (2) with fit parameters p_0-p_3 [4].

$$\mathrm{RBE}\left(D_p, [\alpha/\beta]_x, LET_d\right) = \frac{1}{2\mathrm{D_p}\left(\sqrt{[\alpha/\beta]_\mathrm{x}^2 + 4[\alpha/\beta]_\mathrm{x}\alpha[\mathrm{LET_d}]/\alpha_\mathrm{x}\mathrm{D_p} + 4^{\beta[\mathrm{LET_d}]}/\beta_\mathrm{x}\mathrm{D_p}^2} - [\alpha/\beta]_\mathrm{x}\right)} \quad (1)$$

$$RBE\left(D_p, [\alpha/\beta]_x, LET_d\right) = \frac{1}{2D_p\left(\sqrt{[\alpha/\beta]_x^2 + 4D_p[\alpha/\beta]_x\left[p_0 + \frac{p_1}{(\alpha/\beta)_x}LET_d\right] + 4D_p^2\left[p_2 + p_3\sqrt{\{\alpha/\beta\}}_x LET_d\right]^2} - [\alpha/\beta]_\mathrm{x}\right)} \quad (2)$$

For a 6-MV photon beam, secondary electrons result in an LET of ~0.2 while the LET of protons ranges from ~1–25 in the energy region of interest in PT. With fewer tracks involved for the same dose compared to photons, protons deposit dose more concentrated in space and the clustering of energy deposition mainly in the cellular DNA can result in damage that is more complex and therefore more difficult to repair compared to photon induced damage. The increase in ionization density also causes an increase in reactive oxygen species (ROS) with protons compared to photon radiation [5–7]. The increasing LET with increasing depth of penetration is of particularly concern for critical structures immediately downstream of the target if single-field uniform dose (spread-out Bragg peak, SOBP) is delivered. For multiple fields and particularly in intensity-modulated PT (IMPT) delivering inhomogeneous dose distributions per field, the LET distribution can be highly inhomogeneous. LET values in patients are typically higher than ~10 in the distal fall-off, but only ~2–4 in the center of the target for typical beam arrangements (Figure 1) [8, 9]. Figure 2 shows RBE relationships based on an empirical model deduced from CCS experiments.

The RBE for CCS also depends on the cell line. Differences in DNA damage complexity can be associated with differences in repair pathways such as, for instance, a higher portion of homologous recombination versus non-homologous end-joining with higher LET [10–17]. Higher complexity of DNA damage also leads to slower repair [6]. Furthermore, differences

in foci size comparing photon and proton irradiation at the same dose indicate significant variations in inflammatory response [18–20]. The analysis of experimental in-vitro data show a trend of increasing RBE as $(\alpha/\beta)_x$ decreases, i.e., the RBE for late damage is expected to be higher than for early responding tissues (Figure 2) [21], with $(\alpha/\beta)_x$ indicative of the curvature of the cell survival curve and thus the sensitivity to fractionation.

Furthermore, the RBE for cell survival increases with decreasing dose (Figure 2), which is more pronounced for late responding compared to early responding tissues. A larger dose dependency is predicted for higher values of LET. The dose dependency of the RBE in PT is not well studied experimentally but might be significant for doses below 1 Gy. Note that the linear-quadratic equation might not be valid below ~1 Gy [22, 23] which could affect dose-response estimations for organs at risk typically receiving less than 1 Gy for a 2 Gy per fraction treatment. It may also be questionable (depending on the endpoint) for doses above ~10 Gy [24], which could have implications when considering hypo-fractionated treatment regimens [25–27].

Clonogenic cell survival data and in vivo pathways

It is unclear to what extend these RBE relationships based on CCS should guide clinical practice. Biological mechanisms leading to tumor control or normal tissue toxicities are multifarious and the classical target cell theory [1], which is at the core of the RBE concept, is insufficient to describe effects in patients. Figure 3 schematically and roughly outlines the most relevant aspects. Damage to cells start with either direct or indirect damage that might undergo repair or result in cell inactivation due to apoptotic or necrotic pathways. Due to differences in DNA damage, the ratio of apoptotic versus necrotic pathways likely differs between photon and proton radiation [28]. The diagram is a simplification and disregards many aspects, e.g., cross talks between pathways, programmed necrosis versus secondary necrosis [29], mitotic catastrophe, senescence, autophagy, paraptosis, and other phenomena [30]. For instance, apoptosis and autophagy do contribute to immunogenic response [31] and both necrotic as well as apoptotic pathways may release anti-inflammatory cytokines.

With respect to direct (predominantly apoptotic) cell death in tumors we might in part rely on knowledge gained from in vitro data. However, in addition to cell kill, there can be functional impairment in tumor cells, e.g., loss of proliferation while maintaining the ability to release antigens. Furthermore, tumor response does depend on the microenvironment [32]. While patient specificity as well as tumor heterogeneity cannot be fully considered in vitro, they are impacting both photon and proton data.

For normal tissues, there is no direct path to early and particularly late toxicities. Radiation causes the activation of cytokine cascades causing radiation protection or sensitization [33]. The complex pathways will depend on the type of DNA damage and impact response differences between protons and photons. In order to understand normal tissue toxicity we need to understand the inactivation of functional organ subunits [34] as well as the distribution of damage in an organ which, due to the difference in integral dose and dose distribution, differs for the two radiation modalities. Normal tissue sensitivity is determined by tissue organization of these subunits leading to a distinction between parallel and serial

organs [35]. This is not covered by RBE but should ideally be considered in NTCP (Normal Tissue Complication Probability) models via organ dose distributions, including potential physiological interactions of different organs (e.g., lung and heart) [36, 37].

Furthermore, radiation damage triggers innate and adaptive immune response. Radiation mediated immune response in normal tissue is part of inflammatory pathways that preludes acute normal tissue toxicities as well as late toxicities via chronic inflammation. Radiation can also introduce immune-suppressive effects via detrimental effects on tumor infiltrating lymphocytes, lymphatic vessels and nodes, as well as circulating lymphocytes [38]. Radiation sensitivity (and likely RBE) differs in lymphocyte sub-populations and even by activation status of lymphocytes [39–41]. The lower integral dose with PT reduces the dose to circulating lymphocytes and might cause differences in lymphopenia between PT and photon therapies [42–48].

Finally, damage to endothelial cells impacts the RBE. Effects on small- and medium-sized vessels leads to disruption of the endothelial lining and the vasculature. Changes in endothelial cell phenotypes cause increased vascular permeability and tumor cell death [49–51]. The role of endothelial cells in tumor response is controversial [49, 50, 52–55]. Endothelial cells are generally assumed to be less sensitive compared to tumor cells [56, 57]. The loss of endothelial cells can lead to a decrease in blood perfusion and an increase in hypoxia triggering increased levels of hypoxia inducible factor-1 (HIF-1) which promotes neovascularization [58, 59]. Vascular abnormalities as presented in tumors negatively impact immune response [60] and damage-associated molecular patterns (DAMPs) activate the innate immune system via endothelial cell activation [61].

In normal tissues, capillaries present the most radiosensitive vessels because the single layer of endothelium is susceptible to ionizing radiation [62]. In addition to cell kill, radiation leads to endothelial cell activation involving expression of cytokines, chemokines and adhesion molecules facilitating recruitment and attachment of circulating leukocytes on the vascular wall [63]. Adhesion molecules are mediators of inflammatory reactions as their expression leads to increased recruitment of immune cells. A higher LET is likely more effective in triggering endothelial cell adhesiveness leading to increased vascular permeability.

In summary, tumor control and normal tissue complications caused by radiation are a combination of four aspects of which only the first two are related to CCS:

- **a.** direct cellular effects: clonogenic cell death of tumor cell populations and normal tissue cell populations that act as functional subunits
- **b.** direct cellular functional effects: inactivation of tumor cell populations or compromising the functionality of functional subunits in normal tissue
- **c.** indirect effects: vascular disruption due to endothelial cell death/damage
- **d.** indirect systemic effects: antigen release, cytokine/chemokine activation, as well as radiation induced immune cell death

Tumor RBE

Clinically applied values of $(\alpha/\beta)_x$ are a surrogate for all the mechanisms shown in figure 3 and are based on empirical evidence and data extracted from patient cohorts by fitting $(\alpha/\beta)_x$ dependent TCP (Tumor Control Probability) models to tumor growth or by comparing outcome of different fractionation regimens. Taking these $(\alpha/\beta)_x$ values [64–67], and assuming that RBE as a function of $(\alpha/\beta)_x$ follows the same trend as the one seen in CCS (Figure 2), leads to predicted RBE values shown in figure 4 for LET=2 (indicative of a typical lower boundary for the target), LET=4 (indicative of a typical average for the target), and LET=10 (indicative of a typical maximum for the target). Note that these absolute RBE values are model dependent and reflect predictions by the model shown in equation (2). However, the overall trend holds for all RBE models.

The $(\alpha/\beta)_x$ from in vitro measurements are not one-to-one related to $(\alpha/\beta)_x$ extracted from clinical data. Whether in vitro measurements translate to clinically used $(\alpha/\beta)_x$ depends on the tumor histology and site, e.g., tumor types can have different $(\alpha/\beta)_x$ values depending on the tumor microenvironment (e.g., adenocarcinoma of the breast and prostate [65]). Table 1 compares RBE values shown in figure 4 with those from CCS in vitro.

Breast:

Clinical data result in $(\alpha/\beta)_x$ of 2.2–4.6 Gy (4.0–4.4 Gy for adenocarcinoma). Using an empirical model, this corresponds to minimum RBE values for breast tumors between 1.08 and 1.18 in areas of low LET. For comparison, CCS results in the middle of an SOBP showed an RBE of 0.93 [15].

CNS - Head and Neck:

For CNS tumors the literature reports $(\alpha/\beta)_x$ between 1.8 and 12.5 Gy (2.4 Gy for chordoma, 3.1–12.5 Gy for glioma, 3.3–3.8 Gy for meningioma, and 1.8–2.4 Gy for vestibular schwannoma). For other head and neck tumors, $(\alpha/\beta)_x$ from negative values to 30 Gy were deduced from clinical data, the majority on squamous cell carcinoma. The large spread is reflected in the outliers in predicted RBE values seen in figure 4.

Indicative of potential minimum RBE in a tumor, in vitro data at low LET have been reported for various cell lines. For human salivary gland tumors cells, RBE values were reported as ~1.0 and ~1.1 at LET of ~2 [21]. For squamous cell carcinoma, RBE=1.4 (LET=2) [21] and RBE=1.0 (LET=2.1) [68] have been measured. RBE values for SQ20B derived from human epithelium tumors of the larynx translate into an RBE of ~1.2 (LET=2.4) [21] whereas Hep2 cells from a squamous carcinoma of the larynx showed RBE values of ~1.4 for LET of ~2.7 [21]. SCC25 derived from human epithelium tumors of the tongue showed an RBE of ~0.9 (LET=1.9) [21]. Three HPV-negative squamous cell carcinoma cell lines and 3 HPV-positive cell lines were studied with RBE values ranging from 1.15 to 1.33 in the center of an SOBP [69]. Using 3D cell cultures an RBE ~1.15 was measured for head neck squamous cell carcinoma at LET=3.7 [70]. With respect to expected maximum RBE values, measurements on SQ20B derived from human epithelium tumors of the larynx translate to RBE of ~1.25 (LET=7) and ~1.05 (LET=7.7) [21]. Furthermore,

Hep2 cells from a squamous carcinoma of the larynx showed RBE values of ~2.1 for LET=8.7 and SCC25 derived from human epithelium tumors of the tongue showed RBE of ~2.1 (LET=8.9) [21]. In vitro measurements using glioma (U87) resulted in RBE of ~1.35 at LET=2.6 [71] and 1.1 at LET=2.26 (T98) [72]. Related to potential maximum target RBE values, the same studies report an RBE of ~1.7 at LET=13.4 (U87) and RBE =1.7–1.8 at ~7.3 (T98). For seven different glioblastoma cell lines RBE values between ~0.8 and ~1.3 were deduced [73] (no LET reported) as well as an RBE of >2.0, albeit at an LET of 6.2 [21].

Gastrointestinal:

Clinical data suggest $(\alpha/\beta)_x$ values of 13.4 Gy and 4.9 Gy for liver and esophagus, respectively. In the middle of an SOBP, RBE values for eight human HCC cell lines have been measured in vitro revealing large variations [17]. RBE values for 1.8 Gy/fraction were between 1 and 1.56 (at >2Gy; no $(\alpha/\beta)_x$ values reported). RBE values for human esophageal adenocarcinoma cell lines as well as squamous cell carcinoma cell lines were also measured in vitro [74]. For the two adenocarcinoma cell lines RBE values were not statistically different from 1.0 (at >2Gy; no $(\alpha/\beta)_x$ values reported). The difference between the squamous cell carcinoma cell lines was substantial with RBE values of 2.27 and 0.70. Using 3D cell cultures, large variations in RBE amongst six pancreatic duct adenocarcinoma cell lines were measured (RBE ~0.7 to ~2.4; no $(\alpha/\beta)_x$ reported) [75].

Genitourinary:

Data for adenocarcinoma of the prostate show $(\alpha/\beta)_x$ between 0 and 20 Gy from 63 different studies (50 of which showed values between 0 and 5 Gy). For cervix, $(\alpha/\beta)_x$ values deduced from clinical data range from 10 to 52.6 Gy, whereas $(\alpha/\beta)_x$ between 2.7 and 11.1 Gy were deduced for rectum, and 13–24 Gy for bladder.

Measured RBE values in vitro for the DU-145 prostate cancer cell line were low with ~1.0 at LET=2.9 [21]. Other studies using DU-145 found RBE values of ~1.83 at LET=1.9 [76] and ~1.85 at LET=1.9 [68], respectively. Representative for the distal part of the target, RBE values of ~1.98 at LET=4.1 [76] and ~2.08 at LET=4.5 [68] were reported. Furthermore, an RBE of 1.21 was deduced for colon carcinoma at 3.71 [21]. In vitro data for colorectal tumor cells report RBE values below <1.0 even for LET=7.7 and data for cervix predict an RBE of 1.07 and 1.28 at LET=2.4 and 6.9, respectively [21].

Sarcoma:

Clinical data from liposarcoma indicate a low $(\alpha/\beta)_x$ of 0.4 Gy suspecting a high RBE while in vitro data show an RBE of 1.02 for LET=2.56 [21].

Thoracic:

Large variation in $(\alpha/\beta)_x$ for NSCLC deduced from clinical data (3.9–8.2 Gy) as well as large variations in RBE in vitro have been shown. For A549 and H460 NSCLC cell lines, RBE values of 1.3 and 1.37 were reported for an LET of 2.5 [21]. Another study measured an RBE of 1.14 for A549 (LET=2.26) [72]. RBE values in the middle of an SOBP for SF=0.5 were measured for 17 different NSCLC cell lines in vitro with values between

0.97 and 1.77 [15]. In three of these cell lines, the increased RBE was correlated with alterations in the BRCA/Fanconi Anemia DNA repair pathway. In Calu-6, the data suggested the presence of a FANCD2 pathway defect leading to a previously unreported persistence of RAD51 foci after proton irradiation compared to the photon reference radiation. As for potential maximum RBE values in the target, A549 RBE of ~2.3 was reported for an LET of 10 [21] and an RBE of 1.45–2.31 for A549 was seen for LET=7.3 [72].

Pediatric:

Clinical data from rhabdomyosarcoma indicate an $(\alpha/\beta)_x$ of 2.8 Gy. As medulloblastoma are expected to have a higher $(\alpha/\beta)_x$ it was speculated that the RBE for medulloblastoma might be <1.1 potentially leading to failure in tumor control [77–79]. In a retrospective review of 109 patients with medulloblastoma treated with PT, no statistically significant correlation between areas of low LET (indicative of low RBE) and regions of recurrence was found, and patterns of failure did not differ from patients treated with photons [79]. Experimental in vitro data on cell survival of medulloblastoma cells report an RBE of 1.13 (LET=2.2) [21].

Normal tissue RBE

To ensure target coverage, the distal edge of a SOBP (in single field uniform dose delivery) extends beyond the tumor/CTV and therefore into normal tissue. While the beamlet distribution in IMPT causes a more complex plan optimization dependent LET distribution, elevated LET values would still occur mostly in the vicinity of the target contour (see Figure 1). Furthermore, considering typically lower $(\alpha/\beta)_x$ for normal tissues combined with lower doses compared to the target, one might expect larger RBE values when considering toxicities compared to tumor control. Tissues with high mitotic activity and rapid turnover and cycling stem/progenitor populations might respond early and regenerate more quickly after radiation damage [33]. Those would be expected to have a high α/β, if the α/β of the parenchyma alone is used to parameterize tissue response. In contrast, tissues with slow turnover might respond late and may rely more on proliferation and reprogramming of mature cells instead of cycling stem/progenitor populations [33]. Table 2 summarizes $(\alpha/\beta)_x$ values estimated from human data and figure 5 shows the RBE as a function of $(\alpha/\beta)_x$ from CCS. A figure similar to figure 4 for normal tissue is not meaningful. First, $(\alpha/\beta)_x$ from human data are based on fairly homogenous photon dose distributions in the region of interest. For more heterogeneous proton dose distributions the RBE has to be assigned on a voxel-by-voxel basis. Second, while in the case of tumor control, there is one direct pathway from cell survival to tumor cell reduction, normal tissue damage starts with damage to functional subunits leading to early and late toxicity (Figure 3). Furthermore, endothelial cells are organ specific, e.g., brain endothelial cells promote the blood brain barrier while capillary endothelial cells of the kidney allow blood filtration. The radiosensitivity of endothelial cells does depend on the organ with the turnover time of endothelial cells in an organ not necessarily related to the turnover time of the parenchyma [80].

Breast:

In breast, no relation has been found between fibroblast radiosensitivity and the development of late normal tissue effects such as fibrosis, demonstrating the limitation of the target-cell

hypothesis [81, 82]. Breast treatments often include a significant portion of the heart, which might lead to fibrosis and coronary heart disease, typically starting with microvascular injury inducing ischemia. Long term follow-up is needed to assess effects of potentially elevated RBE values. A randomized trial comparing proton and photon treatments is currently ongoing (NCT02603341).

A retrospective analysis of late-phase lung-density changes (indicative of asymptomatic fibrosis) for a small cohort of breast cancer patients irradiated to the chest wall showed that late-phase asymptomatic radiographic changes on follow-up CTs in the lung are associated with RBEs potentially even exceeding 3.0 [83]. When patients receive PT for breast cancer, ribs located in the distal region of the proton field may receive higher effective doses. An increased rib fracture rate of 7% was seen in PT for breast cancer. The LET in fractured areas was increased to ~6 suggesting that there is an end-of-range radiobiological effect and the RBE-weighted dose could be 20–30% higher than expected from RBE=1.1 [84]. Furthermore, in re-irradiation of locally recurrent breast cancer patients a higher rate of acute grade 3–4 skin toxicity and chest wall infections was seen with protons [85]. This seems likely a dosimetric rather than an RBE effect. Clonogenic cell survival suggest RBE values in skin fibroblasts between 1.4 and 2.2 at LET between 2 and 2.6 [21, 71, 86]. The RBE for skin keratinocytes at LET=2.1 was found to be 0.96 [68].

CNS - Head and Neck:

Brain injuries are caused by both vascular damage (vascular hypothesis), damage to glial cells (particularly oligodendrocytes and neurons; glial hypothesis) as well as interactions between the two [87, 88]. Injury to endothelial cells leads to vessel wall necrosis, loss of capillary vasculature and increasing permeability impacting the blood brain barrier which in turn may lead to vascular edema and hypoxia. This is a first step towards brain injuries [89]. Furthermore, regional differences in radiation sensitivity for white or gray matter or other areas of the brain might have implications with the more inhomogenous dose distribution offered by PT.

Neurocognitive toxicities are expected to be lower with protons due to the reduced integral dose [90]. Late contrast-enhancing brain lesions are indicative of a compromised blood-brain barrier. In six glioma patients, a logistic regression model presenting the probability of magnetic resonance (MR) image changes showed a better correlation when LET, as a variable, was included in addition to dose [91]. Numerous studies on temporal lobe necrosis after PT report incidence rates between 5.6 and 17.1% [92–95], i.e., slightly higher than comparable photon data [92]. Based on 110 low-grade glioma patients treated with PT, a voxel-based predictive model was developed for the occurrence of late MR contrast-enhancing lesions and was extrapolated to a patient-level risk model [96, 97]. A cross-validated voxel-level logistic regression to predict local risk for image change was used and predicted a threefold increased risk in the region around the ventricular system and an LET-dependent RBE of 1.22 (LET=2). A strong dependence on LET and an increased RBE for the ventricular proximity was seen even in regions of low LET. Another study on radiographic changes after PT for nasopharyngeal carcinoma estimated that an RBE~1.18 at $D_{1\%}$ [98]. In another study, the relationship between regions of elevated LET

has been assessed for adult brain and head & neck patients and LET was not found to correlate with a risk of brain necrosis. It was concluded that RBE effects might be small compared to inter-patient variability of radiosensitivity and might be obscured by other confounding factors [99]. The complex relationships between vascular and glial mechanisms and their dose-volume effects likely contributes to this finding. Necrosis is likely correlated geometrically with the vascular structure and not only with direct cell kill to the brain parenchyma. Interestingly, there is a statistically significant difference in dose-response for brain necrosis depending on whether tumors are intra- or extracranial [100], emphasizing the importance of vascular effects.

A study in 100 glioma patients showed that the characteristics of pseudo-progression after PT differed from those observed after photon therapy [101]. Not only was the appearance different on MRI, also the timing was different as pseudo-progression after PT developed later compared to photons therapy (15 versus 3 months). Furthermore, there was an affinity for white matter with protons. The authors speculate that an increased RBE at the end of range might play a role.

Other toxicities of interest in head & neck cancer patients include xerostomia and dysphagia. These have been used as examples for model-based trials in PT [102]. Such efforts also aim at enriching patients for improvements in current photon based NTCP models and may allow future RBE estimates. Considering organ dose distribution is warranted. For instance, stem cells of parotid glands are predominantly located in the larger ducts [103].

Gastrointestinal:

Toxicities in the liver originate from damage to the parenchyma (hepatocytes) and to endothelial cells. Various imaging techniques have been used to study differences in radiation induced liver disease between protons and photon treatments. A study using SPECT/CT demonstrated that RBE might differ not only by patient but by baseline liver function [104]. Rib fracture also play a role in hepatocellular carcinoma [105]. A clinical trial comparing PT with IMRT for locally advanced esophageal cancers (NCT01512589) showed a significant reduction of toxicities using protons due to favorable dose distributions [106]. Such studies are not designed to deduce normal tissue RBE.

Genitourinary:

Subregions in the urethra and bladder have been shown to be more predictive for urinary toxicity than the dose to the whole bladder [107]. Late effects in the bladder wall or urethra arise from epithelial and microvascular alterations. A large trial comparing PT and IMRT for low or intermediate risk prostate cancer might ultimately provide RBE estimates (NCT01617161). Several large retrospective studies did not report significant differences in toxicities between the two modalities [108].

Sarcoma:

In bone sarcoma, radiation induced decrease in bone density can lead to fractures. Furthermore, a reduction in bone vascularity combined with impaired bone formation from irradiated osteoblasts affects fracture healing. Evidence suggests that bone fractures are

impacted by elevated LET values with an estimate RBE at the end of range of 1.2–1.3 in ribs [84]. Fractures also occur in radiation treatment for soft tissue sarcoma but no comparative data have been published.

Thoracic:

The capillary endothelium is considered the initial site of pulmonary damage. Radiation pneumonitis leads to vascular permeability, hypoxia, and interstitial edema followed by fibrosis. The killing of fibroblasts leads to increased collagen production and density change. While vascular damage is generally more impactful in small vessels, a role for the major bronchi or associated large pulmonary vessels in the development of severe toxicity was suggested when small volumes of lung are irradiated with high doses [109]. Secondary to reduced vascular capacity in the irradiated region, vasculature in non-irradiated lung regions can be damaged due to enhanced pressure and overload [110]. These effects are important for integral dose considerations.

A retrospective analyses of late-phase lung-density changes in breast cancer patients irradiated to the chest wall showed that late-phase asymptomatic radiographic changes in the lung are associated with an elevated RBE [83]. In contrast, for the same endpoint, an RBE ~1.1 was deduced in a cohort of SBRT lung cancer patients indicating significantly lower RBE at higher doses per fraction. Differences in the time course of the inflammatory response after proton compared to photon SBRT were seen (inflammation occurred earlier in PT) [111]. A study using FDG-PET demonstrated that, despite significantly different dose distributions for IMRT and PT, the slope of the dose linear regression line associated with radiation pneumonitis did not differ and patients who developed pneumonitis had statistically significantly higher mean lung dose and higher slope regardless of treatment modality [112]. A randomized clinical trial comparing toxicities such as pneumonitis from PT versus IMRT (NCT00915005) for NSCLC did not find a benefit of PT [113]. The main reason might be the distribution of dose [114] and regional differences of radiation sensitivity [115]. In studies in NSCLC patients, non-cancer mortality was associated with irradiation of upper regions of the heart, including big vessels (e.g., the vena cava and coronary arteries) and the right atrium [116, 117]. The differences in dose distribution from photon and proton treatments might be more impactful than RBE effects.

Reported dose response data for CCS using human fibroblasts and epithelial cells derived from a lung fibroblast show high $(\alpha/\beta)_x$, i.e., RBE values independent of dose of ~1.16 even at 7.7 [21].

Pediatric:

There is concern that elevated RBE for normal tissue injuries may lead to not only more but also more severe toxicities than expected based on dosimetric indices in pediatric patients [118]. Concerns focus mainly on the occurrence of brainstem necrosis in posterior fossa tumors [118–120]. Low necrosis rates of 1.1% [121] and 0.7% [122] were reported for pediatric low-grade glioma and 166 pediatric patients with CNS malignancies, respectively. Similarly, the incidence of brainstem injury in pediatric patients with posterior fossa tumors was reported as < 2% [123]. Another study reported symptomatic radiation-induced necrosis

in pediatric brain tumor patients as 7% [124]. These numbers seem lower than what would be expected from photon treatments. Others reported a significantly higher incidence of radiographic changes (potentially necrosis) with protons at 31% [120] and, specific for pediatric ependymoma patients, 43% versus 17% in IMRT [125]. A study of 30 PT pediatric brain tumor patients reported 23% radiographic image changes [126]. A comprehensive analysis of childhood cancer survivors and CNS injuries showed a comparatively low necrosis risk of ~5% for pediatric PT [127]. Some studies demonstrate higher correlation of dose with image changes if an LET based correction is employed [126, 128]. The 5-year cumulative incidence of CNS injury for medulloblastoma patients receiving posterior fossa boost fields ranging out in the brainstem was 4% [129]. A total of 10 discrete areas of treatment change were contoured. Eight of these areas had higher LET values than the target, but with the average LET for these areas being 2.7 versus 2.4 in the target area, the difference is likely too small to indicate a correlation with RBE. The significant variations in numerous studies are due to small single institution cohorts and due to the definition of radiographic changes versus necrosis [118]. Presumably, areas of increased RBE had an impact only in those patients that were genetically prone to increased radiosensitivity.

The vasculature in children is likely more radiosensitive leading to vasculopathy [130]. A study in pediatric craniopharyngioma patients treated with PT showed a significant correlation with LET in vascular structures, while no correlation was found with dosimetric parameters alone [131]. On the other hand, in 644 pediatric PT patients with brain and skull base tumors, the 3-year cumulative rates of any vasculopathy and serious vasculopathy were 6.4% and 2.6%, respectively [130]. The data did not suggest rates that are higher in PT compared to photon therapy. The same conclusion can be drawn from a study on cerebral vasculopathy and microbleeds in pediatric brain tumor patients treated with PT [132, 133]. Such imaging studies may miss damage to small vessels or more long-term occurrences of vasculopathy.

Clinical comparison between the two modalities typically prevents distinction between effects due to RBE or due to dose distribution differences. For instance, a study on craniopharyngioma patients treated with protons and IMRT did find a difference in visual defects (52% versus 81% for proton and photon therapy, respectively) [134]. The same holds, for instance, for studies on intellectual outcomes demonstrating superiority of PT [135].

Conclusions

The combined effects of radiation action on tumor cells, tumor vasculature as well as systemic effects of radiation make it difficult to define tumor specific ‘clinical’ RBE values. Tumor dose prescriptions in PT are therefore based on a conservative RBE of 1.1. Potentially, slightly lower values could be encountered in proximal parts of the tumor volume for a given beam direction or for some hypo-fractionated regimen. While, for now, a conservative RBE is appropriate for prescription doses, more realistic RBE estimates should be applied when retrospectively analyzing outcome data. RBE values higher than 1.1 can be expected in the distal part of the tumor in SOBP fields if the relationship of RBE as a function of $(\alpha/\beta)_x$ as deduced from CCS holds for $(\alpha/\beta)_x$ deduced from

clinical data. Furthermore, the average RBE across most tumors volume likely exceeds 1.1. The clinical relevance depends on the sigmoid dose-response curve. Ongoing large clinical trials offer the potential to deduce α/β for tumors treated with protons and might allow adjusting photon-based TCP models with an RBE defined by a shift in D_{50}. Additional studies on genomically characterized human cancer cell lines together with measurements of tumor control using human tumor cells implanted in immune-deficient animals would be valuable. Patient-derived organoids will play a big role as well [136]. While the current concept of RBE aims at population average treatment planning decisions, it is desirable to define biomarkers to identify patients that benefit most from PT. Efforts are ongoing to identify deficiencies in repair pathways. Functional biomarkers, such as foci size of DNA double-strand break markers signaling unrepaired clustered damage, may identify human tumors with increased sensitivity to proton radiation for treatment with radiation alone or in combination with targeted therapies [17, 70, 75, 137]. Radiation therapy is often used in combination with chemotherapies, targeted agents and immune therapies, all of which influence the RBE. For the latter, the impact of radiation dose distributions on the lymphatic system and lymphocytes as well as on immune-related signaling by normal tissues around the tumor needs to be better understood.

An RBE of 1.1 is currently also applied for normal tissue constraints. Even though one would expect smaller variations in the underlying cell population for normal tissues as compared to tumors, the mechanisms leading to normal tissue toxicities are more complex due to the variety of toxicities but also due to the potentially higher impact of vascular damage as compared to cell death in the parenchyma. The lower integral dose in PT may not translate into a toxicity advantage depending on how the dose is distributed and depending on normal tissue RBE [108]. The RBE needs to be applied inhomogenously according to the dose distribution and the distribution of functional subunits. Moreover, it is unclear if current NTCP models are applicable because current models are based on fits to clinical data from dosimetrically more homogeneous photon treatments. In this context, dose-response relationships should not be solely analyzed based on organ contours but on sub-regions or even voxel-based [138]. Personalized normal tissue radiosensitivity might be assessed via transcriptome response [139, 140]. Furthermore, the clinical data on normal tissue toxicities reviewed above have limitations not only because of patient variability but also in terms of institutional bias from treatment planning, delivery, or outcome assessment. There have been many planning studies on RBE effects in PT which are not reviewed here [141–152]. Such studies apply empirical models based on CCS and are valuable to indicate general trends and potential impact of RBE variations in normal tissues. Caution is warranted when interpreting these RBE values quantitatively.

This review focuses on biological and clinical aspects of RBE. There have been other reviews focusing more on the physics of proton biology, i.e., the specific impact and calculation of LET as well as the shaping of LET distributions in treatment optimization [2, 153]. With the difficulty to define reliable RBE values for normal tissue complications, a safe strategy might be to maintain current dose constraints but reduce LET in regions of interest via LET based plan optimization [153–157].

Acknowledgments

Funding Statement

This work was supported by the National Institute of Health / National Cancer Institute; U19 CA-21239

References

1. McMahon SJ. The linear quadratic model: Usage, interpretation and challenges. Phys Med Biol 2018;64:01TR01.
2. Kalholm F, Grzanka L, Traneus E, Bassler N. A systematic review on the usage of averaged LET in radiation biology for particle therapy. Radiother Oncol 2021;161:211–221. [PubMed: 33894298]
3. Rørvik E, Fjæra LF, Dahle TJ, et al. Exploration and application of phenomenological RBE models for proton therapy. Phys Med Biol 2018;63 185013. [PubMed: 30102240]
4. McNamara AL, Schuemann J, Paganetti H. A phenomenological relative biological effectiveness (RBE) model for proton therapy based on all published in vitro cell survival data. Phys Med Biol 2015;60:8399–8416. [PubMed: 26459756]
5. Giedzinski E, Rola R, Fike JR, Limoli CL. Efficient production of reactive oxygen species in neural precursor cells after exposure to 250 MeV protons. Radiat Res 2005;164(Pt 2):540–544. [PubMed: 16187784]
6. Vitti ET, Parsons JL. The radiobiological effects of proton beam therapy: Impact on DNA damage and repair. Cancers (Basel) 2019;11:946.
7. Alan Mitteer R, Wang Y, Shah J, et al. Proton beam radiation induces DNA damage and cell apoptosis in glioma stem cells through reactive oxygen species. Sci Rep 2015;5:13961. [PubMed: 26354413]
8. Grassberger C, Trofimov A, Lomax A, Paganetti H. Variations in linear energy transfer within clinical proton therapy fields and the potential for biological treatment planning. Int J Radiat Oncol Biol Phys 2011;80:1559–1566. [PubMed: 21163588]
9. Grassberger C, Paganetti H. Elevated LET components in clinical proton beams. Phys Med Biol 2011;56:6677–6691. [PubMed: 21965268]
10. Girdhani S, Sachs R, Hlatky L. Biological effects of proton radiation: What we know and don't know. Radiat Res 2013;179:257–272. [PubMed: 23373900]
11. Rostek C, Turner EL, Robbins M, et al. Involvement of homologous recombination repair after proton-induced DNA damage. Mutagenesis 2008;23:119–129. [PubMed: 18267950]
12. Grosse N, Fontana AO, Hug EB, e ontana AO, Augsburger MA, Grosse N. Deficiency in homologous recombination renders mammalian cells more sensitive to proton versus photon irradiation. Int J Radiat Oncol Biol Phys 2014;88:175–181. [PubMed: 24239385]
13. Fontana AO, Augsburger MA, Grosse N, et al. Differential DNA repair pathway choice in cancer cells after proton- and photon-irradiation. Radiother Oncol 2015;116:374–380. [PubMed: 26320609]
14. Liu Q, Underwood TSA, Kung J, et al. Disruption of SLX4-MUS81 function increases the relative biological effectiveness of proton radiation. Int J Radiat Oncol Biol Phys 2016;95:78–85. [PubMed: 27084631]
15. Liu Q, Ghosh P, Magpayo N, et al. Lung cancer cell line screen links fanconi anemia/BRCA pathway defects to increased relative biological effectiveness of proton radiation. Int J Radiat Oncol Biol Phys 2015;91:1081–1089. [PubMed: 25832698]
16. Szymonowicz K, Krysztofiak A, Linden JV, et al. Proton irradiation increases the necessity for homologous recombination repair along with the indispensability of non-homologous end joining. Cells 2020;9:889.
17. Choi C, Son A, Lee GH, et al. Targeting DNA-dependent protein kinase sensitizes hepatocellular carcinoma cells to proton beam irradiation through apoptosis induction. PLoS One 2019;14 e0218049. [PubMed: 31194786]

18. Ibañez IL, Bracalente C, Molinari BL, et al. Induction and rejoining of DNA double strand breaks assessed by H2AX phosporylation in melanoma cells irradiated with proton and lithium beams. Int J Radiat Oncol Biol Phys 2009;74:1226–1235. [PubMed: 19545788]
19. Leatherbarrow EL, Harper JV, Cucinotta FA, O'Neill P. Induction and quantification of gamma-H2AX foci following low and high-LET irradiation. Int J Radiat Biol 2006;82:111–118. [PubMed: 16546909]
20. Finnberg N, Wambi C, Ware JH, Kennedy AR, El-Deiry WS. Gamma-radiation (GR) triggers a unique gene expression profile associated with cell death compared to proton radiation (PR) in mice in vivo. Cancer Biol Ther 2008;7:2023–2033. [PubMed: 19106632]
21. Paganetti H Relative biological effectiveness (RBE) values for proton beam therapy. Variations as a function of biological endpoint, dose, and linear energy transfer. Phys Med Biol 2014;59:R419–R472. [PubMed: 25361443]
22. Joiner MC, Lambin P, Malaise EP, et al. Hypersensitivity to very-low single radiation doses: Its relationship to the adaptive response and induced radioresistance. Mutat Res 1996;358:171–183. [PubMed: 8946022]
23. Skarsgard LD, Wouters BG. Substructure in the cell survival response at low radiation dose: effect of different subpopulations. Int J Radiat Biol 1997;71:737–749. [PubMed: 9246187]
24. Kirkpatrick JP, Brenner DJ, Orton OG. Point/counterpoint. The linear-quadratic model is inappropriate to model high dose per fraction in radiosurgery. Med Phys 2009;36:3381–3384. [PubMed: 19746770]
25. Carabe-Fernandez A, Dale RG, Hopewell JW, Jones B, Paganetti H. Fractionation effects in particle radiotherapy: Implications for hypofractionation regimes. Phys Med Biol 2010;55:5685–5700. [PubMed: 20826903]
26. Dasu A, Toma-Dasu I. Impact of variable RBE on proton fractionation. Med Phys 2013;40 011705. [PubMed: 23298075]
27. Holloway RP, Dale RG. Theoretical implications of incorporating relative biological effectiveness into radiobiological equivalence relationships. Br J Radiol 2013;86 20120417. [PubMed: 23385996]
28. Miszczyk J, Rawojć K, Panek A, et al. Do protons and x-rays induce cell-killing in human peripheral blood lymphocytes by different mechanisms? Clin Transl Radiat Oncol 2018;9:23–29. [PubMed: 29594247]
29. Nehs MA, Lin CI, Kozono DE, et al. Necroptosis is a novel mechanism of radiation-induced cell death in anaplastic thyroid and adrenocortical cancers. Surgery 2011;150:1032–1039. [PubMed: 22136818]
30. Broker LE, Kruyt FA, Giaccone G. Cell death independent of caspases: A review. Clin Cancer Res 2005;11:3155–3162. [PubMed: 15867207]
31. Sia J, Szmyd R, Hau E, Gee HE. Molecular mechanisms of radiation-induced cancer cell death: A primer. Front Cell Dev Biol 2020;8:41. [PubMed: 32117972]
32. Barker HE, Paget JT, Khan AA, Harrington KJ. The tumour microenvironment after radiotherapy: mechanisms of resistance and recurrence. Nat Rev Cancer 2015;15:409–425. [PubMed: 26105538]
33. McBride WH, Schaue D. Radiation-induced tissue damage and response. J Pathol 2020;250:647–655. [PubMed: 31990369]
34. Withers H, Taylor JM, Maciejewski B. Treatment volume and tissue tolerance. Int J Radiat Oncol Biol Phys 1988;14:751–759. [PubMed: 3350731]
35. Niemierko A, Goitein M. Modeling of normal tissue response to radiation: The critical volume model. Int J Radiat Oncol Biol Phys 1992;25:135–145.
36. van Luijk P, Novakova-Jiresova A, Faber H, et al. Radiation damage to the heart enhances early radiation-induced lung function loss. Cancer Res 2005;65:6509–6511. [PubMed: 16061627]
37. Nalbantov G, Kietselaer B, Vandecasteele K, et al. Cardiac comorbidity is an independent risk factor for radiation-induced lung toxicity in lung cancer patients. Radiother Oncol 2013;109:100–106. [PubMed: 24044794]
38. Kaur P, Asea A. Radiation-induced effects and the immune system in cancer. Front Oncol 2012;2:191. [PubMed: 23251903]

39. Heylmann D, Ponath V, Kindler T, Kaina B. Comparison of DNA repair and radiosensitivity of different blood cell populations. Sci Rep 2021;11:2478. [PubMed: 33510180]
40. Heylmann D, Rödel F, Kindler T, Kaina BD. Radiation sensitivity of human and murine peripheral blood lymphocytes, stem and progenitor cells. Biochim Biophys Acta 2014;1846:121–129. [PubMed: 24797212]
41. Belka C, Ottinger H, Kreuzfelder E, et al. Impact of localized radiotherapy on blood immune cells counts and function in humans. Radiother Oncol 1999;50:199–204. [PubMed: 10368044]
42. Hammi A, Paganetti H, Grassberger C. Modeling intra-cranial blood flow for simualting dose to lymphocytes in radiation therapy treatment regimens. Phys Med Biol 2019 in preparation.
43. Fang P, Shiraishi Y, Verma V, et al. Lymphocyte-sparing effect of proton therapy in patients with esophageal cancer treated with definitive chemoradiation. Int J Part Ther 2018;4:23–32. [PubMed: 30079369]
44. Ko EC, Benjamin KT, Formenti SC. Generating antitumor immunity by targeted radiation therapy: Role of dose and fractionation. Adv Radiat Oncol 2018;3:486–493. [PubMed: 30370347]
45. Routman DM, Garant A, Lester SC, et al. A comparison of grade 4 lymphopenia with proton versus photon radiation therapy for esophageal cancer. Adv Radiat Oncol 2019;4:63–69. [PubMed: 30706012]
46. Mohan R, Liu AY, Brown PD, et al. Proton therapy reduces the likelihood of high-grade radiation-induced lymphopenia in glioblastoma patients: Phase II randomized study of protons vs photons. Neuro Oncol 2021;23:284–294. [PubMed: 32750703]
47. De B, Ng SP, Liu AY, et al. Radiation-associated lymphopenia and outcomes of patients with unresectable hepatocellular carcinoma treated with radiotherapy. J Hepatocell Carcinoma 2021;8:57–69. [PubMed: 33688489]
48. Lambin P, Lieverse RIY, Eckert F, et al. Lymphocyte-sparing radiotherapy: The rationale for protecting lymphocyte-rich organs when combining radiotherapy with immunotherapy. Semin Radiat Oncol 2020;30:187–193. [PubMed: 32381298]
49. Castle KD, Kirsch DG. Establishing the impact of vascular damage on tumor response to high-dose radiation therapy. Cancer Res 2019;79:5685–5692. [PubMed: 31427377]
50. Garcia-Barros M, Paris F, Cordon-Cardo C, et al. Tumor response to radiotherapy regulated by endothelial cell apoptosis. Science 2003;300:1155–1159. [PubMed: 12750523]
51. Kim SD, Yi JM, Park MT. Irradiated endothelial cells modulate the malignancy of liver cancer cells. Oncol Lett 2019;17:2187–2196. [PubMed: 30675283]
52. Moding EJ, Castle KD, Perez BA, et al. Tumor cells, but not endothelial cells, mediate eradication of primary sarcomas by stereotactic body radiation therapy. Sci Transl Med 2015;7 (278):278ra34.
53. Suit HD, Willers H. Comment on “Tumor response to radiotherapy regulated by endothelial cell apoptosis” (I). Science 2003;302:1894.
54. Brown M, Bristow R, Glazer P, et al. Comment on “Tumor response to radiotherapy regulated by endothelial cell apoptosis”(II). Science 2003;302:1894.
55. Camphausen K, Menard C. Angiogenesis inhibitors and radiotherapy of primary tumours. Expert Opin Biol Ther 2002;2:477–481. [PubMed: 12079484]
56. Park HJ, Griffin RJ, Hui S, Levitt SH, Song CW. Radiation-induced vascular damage in tumors: Implications of vascular damage in ablative hypofractionated radiotherapy (SBRT and SRS). Radiat Res 2012;177:311–327. [PubMed: 22229487]
57. Budach W, Taghian A, Freeman J, Gioioso D, Suit HD. Impact of stromal sensitivity on radiation response of tumors. J Natl Cancer Inst 1993;85:988–993. [PubMed: 8496984]
58. Moeller BJ, Cao Y, Li CY, Dewhirst MW. Radiation activates HIF-1 to regulate vascular radiosensitivity in tumors: role of reoxygenation, free radicals, and stress granules. Cancer Cell 2004;5:429–441. [PubMed: 15144951]
59. Brown JM. Radiation damage to tumor vasculature initiates a program that promotes tumor recurrences. Int J Radiat Oncol Biol Phys 2020;108:734–744. [PubMed: 32473180]
60. Fukumura D, Kloepper J, Amoozgar Z, Duda DG, Jain RK. Enhancing cancer immunotherapy using antiangiogenics: Opportunities and challenges. Nat Rev Clin Oncol 2018;15:325–340. [PubMed: 29508855]

61. Krombach J, Hennel R, Brix N, et al. Priming anti-tumor immunity by radiotherapy: Dying tumor cell-derived DAMPs trigger endothelial cell activation and recruitment of myeloid cells. Oncoimmunology 2019;8 e1523097. [PubMed: 30546963]
62. Venkatesulu BP, Mahadevan LS, Aliru ML, et al. Radiation-induced endothelial vascular injury: A review of possible mechanisms. JACC Basic Transl Sci 2018;3:563–572. [PubMed: 30175280]
63. Hallahan DJ, Kuchibhotla J, Wyble C. Cell adhesion molecules mediate radiation-induced leukocyte adhesion to the vascular endothelium. Cancer Res 1996;56:5150–5155. [PubMed: 8912850]
64. Thames HD Jr, Withers HR, Peters LJ, Fletcher GH. Changes in early and late radiation responses with altered dose fractionation: Implications for dose-survival relationships. Int J Radiat Oncol Biol Phys 1982;8:219–226. [PubMed: 7085377]
65. van Leeuwen CM, Oei AL, Crezee J, et al. The alfa and beta of tumours: A review of parameters of the linear-quadratic model, derived from clinical radiotherapy studies. Radiat Oncol 2018;13:96. [PubMed: 29769103]
66. Thames HD, Bentzen SM, Turesson I, Overgaard M, Van den Bogaert W. Time-dose factors in radiotherapy: A review of the human data. Radiother Oncol 1990;19:219–235. [PubMed: 2281152]
67. Lee SP, Leu MY, Smathers JB, McBride WH, Parker RG, Withers HR. Biologically effective dose distribution based on the linear quadratic model and its clinical relevance. Int J Radiat Oncol Biol Phys 1995;33:375–389. [PubMed: 7673025]
68. Mara E, Clausen M, Khachonkham S, et al. Investigating the impact of alpha/beta and LETd on relative biological effectiveness in scanned proton beams: An in vitro study based on human cell lines. Med Phys 2020;47:3691–3702. [PubMed: 32347564]
69. Wang L, Wang X, Li Y, et al. Human papillomavirus status and the relative biological effectiveness of proton radiotherapy in head and neck cancer cells. Head Neck 2017;39:708–715. [PubMed: 28039958]
70. Meerz A, Deville SS, Müller J, Cordes N. Comparative therapeutic exploitability of acute adaptation mechanisms to photon and proton irradiation in 3D head and neck squamous cell carcinoma cell cultures. Cancers (Basel) 2021;13:1190. [PubMed: 33801853]
71. Chaudhary P, Marshall TI, Perozziello FM, et al. Relative biological effectiveness variation along monoenergetic and modulated bragg peaks of a 62-MeV therapeutic proton beam: A preclinical assessment. Int J Radiat Oncol Biol Phys 2014;90:27–35. [PubMed: 24986743]
72. Howard ME, Beltran C, Anderson S, Tseung WC, Sarkaria JN, Herman MG. Investigating dependencies of relative biological effectiveness for proton therapy in cancer cells. Int J Part Ther 2018;4:12–22. [PubMed: 30159358]
73. Chiblak S, Tang Z, Campos B, et al. Radiosensitivity of patient-derived glioma stem cell 3-dimensional cultures to photon, proton, and carbon irradiation. Int J Radiat Oncol Biol Phys 2016;95:112–119. [PubMed: 26254681]
74. Hartfiel S, Häfner M, Perez RL, et al. Differential response of esophageal cancer cells to particle irradiation. Radiat Oncol 2019;14:119. [PubMed: 31286978]
75. Görte J, Beyreuther E, Danen EHJ, Cordes N. Comparative proton and photon irradiation combined with pharmacological inhibitors in 3D pancreatic cancer cultures. Cancers (Basel) 2020;2:3216.
76. Khachonkham S, Mara E, Gruber S, et al. RBE variation in prostate carcinoma cells in active scanning proton beams: In-vitro measurements in comparison with phenomenological models. Phys Med 2020;77:187–193. [PubMed: 32871460]
77. Jones B, Underwood TS, Dale RG. The potential impact of relative biological effectiveness uncertainty on charged particle treatment prescriptions. Br J Radiol 2011;84(Spec No 1):S61–S69. [PubMed: 22374549]
78. Jones B, Wilson P, Nagano A, Fenwick J, McKenna G. Dilemmas concerning dose distribution and the influence of relative biological effect in proton beam therapy of medulloblastoma. Br J Radiol 2012;85:e912–e918. [PubMed: 22553304]

79. Sethi RV, Giantsoudi D, Raiford M, et al. Patterns of failure after proton therapy in medulloblastoma; linear energy transfer distributions and relative biological effectiveness associations for relapses. Int J Radiat Oncol Biol Phys 2014;88:655–663. [PubMed: 24521681]
80. Park MT, Oh ET, Song MJ, Lee H, Park HJ. Radio-sensitivities and angiogenic signaling pathways of irradiated normal endothelial cells derived from diverse human organs. J Radiat Res 2012;53:570–580. [PubMed: 22843622]
81. Peacock J, Ashton A, Bliss J, et al. Cellular radiosensitivity and complication risk after curative radiotherapy. Radiother Oncol 2000;55:173–178. [PubMed: 10799729]
82. Russell NS, Grummels A, Hart AA, et al. Low predictive value of intrinsic fibroblast radiosensitivity for fibrosis development following radiotherapy for breast cancer. Int J Radiat Biol 1998;73:661–670. [PubMed: 9690684]
83. Underwood TSA, Grassberger C, Bass R, et al. Asymptomatic late-phase radiographic changes among chest-wall patients are associated with a proton RBE exceeding 1.1. Int J Radiat Oncol Biol Phys 2018;101:809–819. [PubMed: 29976493]
84. Wang CC, McNamara AL, Shin J, et al. End-of-range radiobiological effect on rib fractures in patients receiving proton therapy for breast cancer. Int J Radiat Oncol Biol Phys 2020;107:449–454. [PubMed: 32240774]
85. Gabani P, Patel H, Thomas MA, et al. Clinical outcomes and toxicity of proton beam radiation therapy for re-irradiation of locally recurrent breast cancer. Clin Transl Radiat Oncol 2019;19:116–122. [PubMed: 31692702]
86. Marshall TI, Chaudhary P, Michaelidesová A, et al. Investigating the implications of a variable RBE on proton dose fractionation across a clinical pencil beam scanned spread-out Bragg peak. Int J Radiat Oncol Biol Phys 2016;95:70–77. [PubMed: 27084630]
87. Belka C, Budach W, Kortmann RD, Bamberg M. Radiation induced CNS toxicity—molecular and cellular mechanisms. Br J Cancer 2001;85:1233–1239. [PubMed: 11720454]
88. Coderre JA, Morris GM, Micca PL, et al. Late effects of radiation on the central nervous system: Role of vascular endothelial damage and glial stem cell survival. Radiat Res 2006;166:495–503. [PubMed: 16953668]
89. Li YQ, Chen P, Haimovitz-Friedman A, Reilly RM, Wong CS. Endothelial apoptosis initiates acute blood-brain barrier disruption after ionizing radiation. Cancer Res 2003;63:5950–5956. [PubMed: 14522921]
90. Sherman JC, Colvin MK, Mancuso SM, et al. Neurocognitive effects of proton radiation therapy in adults with low-grade glioma. J Neurooncol 2016;126:157–164. [PubMed: 26498439]
91. Eulitz J, Troost EGC, Raschke F, et al. Predicting late magnetic resonance image changes in glioma patients after proton therapy. Acta Oncol 2019;58:1536–1539. [PubMed: 31303083]
92. Kitpanit S, Lee A, Pitter KL, et al. Temporal lobe necrosis in head and neck cancer patients after proton therapy to the skull base. Int J Part Ther 2020;6:17–28. [PubMed: 32582816]
93. McDonald MW, Linton OR, Calley CS. Dose-volume relationships associated with temporal lobe radiation necrosis after skull base proton beam therapy. Int J Radiat Oncol Biol Phys 2015;91:261–267. [PubMed: 25636754]
94. Miyawaki D, Murakami M, Demizu Y, et al. Brain injury after proton therapy or carbon ion therapy for head-and-neck cancer and skull base tumors. Int J Radiat Oncol Biol Phys 2009;75:378–384. [PubMed: 19735866]
95. Santoni R, Liebsch N, Finkelstein DM, et al. Temporal lobe (TL) damage following surgery and high-dose photon and proton irradiation in 96 patients affected by chordomas and chondrosarcomas of the base of the skull. Int J Radiat Oncol Biol Phys 1998;41:59–68. [PubMed: 9588918]
96. Bahn E, Bauer J, Harrabi S, Herfarth K, Debus J, Alber M. Late contrast enhancing brain lesions in proton-treated patients with low-grade glioma: Clinical evidence for increased periventricular sensitivity and variable RBE. Int J Radiat Oncol Biol Phys 2020;107:571–578. [PubMed: 32234554]
97. Bauer J, Bahn E, Harrabi S, Herfarth K, Debus J, Alber M. How can scanned proton beam treatment planning for low-grade glioma cope with increased distal RBE and locally increased

radiosensitivity for late MR-detected brain lesions? Med Phys 2021;48:1497–1507. [PubMed: 33506555]

98. Zhang YY, Huo WL, Goldberg SI, et al. Brain-specific RBE of protons based on long-term outcome of patients with nasopharyngeal carcinoma. Int J Radiat Oncol Biol Phys 2021;110:984–992. [PubMed: 33600889]
99. Niemierko A, Schuemann J, Niyazi M, et al. Brain necrosis in adult patients after proton therapy: Is there evidence for dependency on linear energy transfer (LET)? Int J Radiat Oncol Biol Phys 2021;109:109–119. [PubMed: 32911019]
100. Niyazi M, Niemierko A, Paganetti H, et al. Volumetric and actuarial analysis of brain necrosis in proton therapy using a novel mixture cure model. Radiother Oncol 2020;142:154–161. [PubMed: 31563411]
101. Ritterbusch R, Halasz LM, Graber JJ. Distinct imaging patterns of pseudoprogression in glioma patients following proton versus photon radiation therapy. J Neurooncol 2021;152:583–590. [PubMed: 33751335]
102. Langendijk JA, Lambin P, De Ruysscher D, Widder J, Bos M, Verheij M. Selection of patients for radiotherapy with protons aiming at reduction of side effects: The model-based approach. Radiother Oncol 2013;107:267–273. [PubMed: 23759662]
103. van Luijk P, Pringle S, Deasy JO, et al. Sparing the region of the salivary gland containing stem cells preserves saliva production after radiotherapy for head and neck cancer. Sci Transl Med 2015;7:305ra147.
104. Price RG, Apisarnthanarax S, Schaub SK, et al. Regional radiation dose-response modeling of functional liver in hepatocellular carcinoma patients with longitudinal sulfur colloid SPECT/CT: A proof of concept. Int J Radiat Oncol Biol Phys 2018;102:1349–1356. [PubMed: 29932945]
105. Kanemoto A, Mizumoto M, Okumura T, et al. Dose-volume histogram analysis for risk factors of radiation-induced rib fracture after hypofractionated proton beam therapy for hepatocellular carcinoma. Acta Oncol 2013;52:538–544. [PubMed: 22950386]
106. Lin SH, Hobbs BP, Verma V, et al. Randomized phase IIB trial of proton beam therapy versus intensity-modulated radiation therapy for locally advanced esophageal cancer. J Clin Oncol 2020;38:1569–1579. [PubMed: 32160096]
107. Mylona E, Ebert M, Kennedy A, et al. Rectal and urethro-vesical subregions for toxicity prediction after prostate cancer radiation therapy: Validation of voxel-based models in an independent population. Int J Radiat Oncol Biol Phys 2020;108:1189–1195. [PubMed: 32673785]
108. Prasanna PG, Rawojc K, Guha C, Buchsbaum JC, Miszczyk JU, Coleman CN. Normal tissue injury induced by photon and proton therapies: Gaps and opportunities. Int J Radiat Oncol Biol and Phys 2021;110:1325–1340. [PubMed: 33640423]
109. Stam B, Kwint M, Guckenberger M, et al. Subgroup survival analysis in stage I-II NSCLC patients with a central tumor partly treated with risk-adapted SBRT. Int J Radiat Oncol Biol Phys 2019;103:132–141. [PubMed: 30176275]
110. Ghobadi G, Bartelds B, van der Veen SJ, et al. Lung irradiation induces pulmonary vascular remodelling resembling pulmonary arterial hypertension. Thorax 2011;67:334–341. [PubMed: 22201162]
111. Li Y, Dykstra M, Best TD, et al. Differential inflammatory response dynamics in normal lung following stereotactic body radiation therapy with protons versus photons. Radiother Oncol 2019;136:169–175. [PubMed: 31015121]
112. Shusharina N, Liao Z, Mohan R, et al. Differences in lung injury after IMRT or proton therapy assessed by (18)FDG PET imaging. Radiother Oncol 2018;128(1):147–153. [PubMed: 29352608]
113. Liao Z, Lee JJ, Komaki R, et al. Bayesian adaptive randomization trial of passive scattering proton therapy and intensity-modulated photon radiotherapy for locally advanced non-small-cell lung cancer. J Clin Oncol 2018;36:1813–1822. [PubMed: 29293386]
114. Palma G, Monti S, Xu T, et al. Spatial dose patterns associated with radiation pneumonitis in a randomized trial comparing intensity-modulated photon therapy with passive scattering

proton therapy for locally advanced non-small cell lung cancer. Int J Radiat Oncol Biol Phys 2019;104:1124–1132. [PubMed: 30822531]

115. Kocak Z, Borst GR, Zeng J, et al. Prospective assessment of dosimetric/physiologic-based models for predicting radiation pneumonitis. Int J Radiat Oncol Biol Phys 2007;67:178–186. [PubMed: 17189069]
116. Stam B, Peulen H, Guckenberger M, et al. Dose to heart substructures is associated with non-cancer death after SBRT in stage I-II NSCLC patients. Radiother Oncol 2017;123:370–375. [PubMed: 28476219]
117. McWilliam A, Khalifa J, Vasquez Osorio E, et al. Novel methodology to investigate the effect of radiation dose to heart substructures on overall survival. Int J Radiat Oncol Biol Phys 2020;108:1073–1081. [PubMed: 32585334]
118. Haas-Kogan D, Indelicato D, Paganetti H, et al. National Cancer Institute workshop on proton therapy for children: Considerations regarding brainstem injury. Int J Radiat Oncol Biol Phys 2018;101:152–168. [PubMed: 29619963]
119. Yock TI, Bhat S, Szymonifka J, et al. Quality of life outcomes in proton and photon treated pediatric brain tumor survivors. Radiother Oncol 2014;113:89–94. [PubMed: 25304720]
120. Kralik SF, Ho CY, Finke W, et al. Radiation necrosis in pediatric patients with brain tumors treated with proton radiotherapy. AJNR Am J Neuroradiol 2015;36:1572–1578. [PubMed: 26138138]
121. Indelicato DJ, Rotondo RL, Uezono H, et al. Outcomes following proton therapy for pediatric low-grade glioma. Int J Radiat Oncol Biol Phys 2019;104:149–156. [PubMed: 30684665]
122. Vogel J, Grewal A, O'Reilly S, et al. Risk of brainstem necrosis in pediatric patients with central nervous system malignancies after pencil beam scanning proton therapy. Acta Oncol 2019;58:1752–1756. [PubMed: 31512931]
123. Gentile MS, Yeap BY, Paganetti H, et al. Brainstem injury in pediatric patients with posterior fossa tumors treated with proton beam therapy and associated dosimetric factors. Int J Radiat Oncol Biol Phys 2018;100:719–729. [PubMed: 29413284]
124. Bojaxhiu B, Ahlhelm F, Walser M, et al. Radiation necrosis and white matter lesions in pediatric patients with brain tumors treated with pencil beam scanning proton therapy. Int J Radiat Oncol Biol Phys 2018;100:987–996. [PubMed: 29485079]
125. Gunther JR, Sato M, Chintagumpala M, et al. Imaging changes in pediatric intracranial ependymoma patients treated with proton beam radiation therapy compared to intensity modulated radiation therapy. Int J Radiat Oncol Biol Phys 2015;93:54–63. [PubMed: 26279024]
126. Roberts KW, Wan Chan Tseung HS, Eckel LJ, Harmsen WS, Beltran C, Laack NN. Biologic dose and imaging changes in pediatric brain tumor patients receiving spot scanning proton therapy. Int J Radiat Oncol Biol Phys 2019;105:664–673. [PubMed: 31301328]
127. Mahajan A, Stavinoha PL, Rongthong W, et al. Neurocognitive effects and necrosis in childhood cancer survivors treated with radiation therapy: A PENTEC comprehensive review [e-pub ahead of print]. Int J Radiat Oncol Biol Phys 2021 2021. 10.1016/j.ijrobp.2020.11.073. accessed August 22, 2021.
128. Peeler CR, Mirkovic D, Titt U, et al. Clinical evidence of variable proton biological effectiveness in pediatric patients treated for ependymoma. Radiother Oncol 2016;121:395–401. [PubMed: 27863964]
129. Giantsoudi D, Sethi RV, Yeap BY, et al. Incidence of CNS injury for a cohort of 111 patients treated with proton therapy for medulloblastoma: LET and RBE associations for areas of injury. Int J Radiat Oncol Biol Phys 2016;95:287–296. [PubMed: 26691786]
130. Hall MD, Bradley JA, Rotondo RL, et al. Risk of radiation vasculopathy and stroke in pediatric patients treated with proton therapy for brain and skull base tumors. Int J Radiat Oncol Biol Phys 2018;101:854–859. [PubMed: 29730064]
131. Bolsi A, Placidi L, Pica A, et al. Pencil beam scanning proton therapy for the treatment of craniopharyngioma complicated with radiation-induced cerebral vasculopathies: A dosimetric and linear energy transfer (LET) evaluation. Radiother Oncol 2020;149:197–204. [PubMed: 32387488]

132. Kralik SF, Watson GA, Shih CS, Ho CY, Finke W, Buchsbaum J. Radiation-induced large vessel cerebral vasculopathy in pediatric patients with brain tumors treated with proton radiation therapy. Int J Radiat Oncol Biol Phys 2017;99:817–824. [PubMed: 28867358]
133. Kralik SF, Mereniuk TR, Grignon L, et al. Radiation-induced cerebral microbleeds in pediatric patients with brain tumors treated with proton radiation therapy. Int J Radiat Oncol Biol Phys 2018;102:1465–1471. [PubMed: 30092336]
134. Bishop AJ, Greenfield B, Mahajan A, et al. Proton beam therapy versus conformal photon radiation therapy for childhood craniopharyngioma: Multi-institutional analysis of outcomes, cyst dynamics, and toxicity. Int J Radiat Oncol Biol Phys 2014;90:354–361. [PubMed: 25052561]
135. Kahalley LS, Peterson R, Ris MD, et al. Superior intellectual outcomes after proton radiotherapy compared with photon radiotherapy for pediatric medulloblastoma. J Clin Oncol 2020;38:454–461. [PubMed: 31774710]
136. Sachs N, Clevers H. Organoid cultures for the analysis of cancer phenotypes. Curr Opin Genet Dev 2014;24:68–73. [PubMed: 24657539]
137. Kageyama SI, Junyan D, Hojo H, et al. PARP inhibitor olaparib sensitizes esophageal carcinoma cells to fractionated proton irradiation. J Radiat Res 2020;61:177–186. [PubMed: 31976528]
138. Palma G, Monti S, Conson M, Pacelli R, Cella L. Normal tissue complication probability (NTCP) models for modern radiation therapy. Semin Oncol 2019;46:210–218. [PubMed: 31506196]
139. Nowrouzi A, Sertorio MG, Akbarpour M, et al. Personalized assessment of normal tissue radiosensitivity via transcriptome response to photon, proton and carbon irradiation in patient-derived human intestinal organoids. Cancers (Basel) 2020;12:469.
140. Sertorio M, Nowrouzi A, Akbarpour M, et al. Differential transcriptome response to proton versus x-ray radiation reveals novel candidate targets for combinatorial PT therapy in lymphoma. Radiother Oncol 2021;155:293–303. [PubMed: 33096164]
141. Liu C, Zheng D, Bradley JA, et al. Incorporation of the LETd-weighted biological dose in the evaluation of breast intensity-modulated proton therapy plans. Acta Oncol 2021;60:252–259. [PubMed: 33063569]
142. Marteinsdottir M, Wang CC, McNamara AL, Depauw N, Shin J, Paganetti H. The impact of variable RBE in proton therapy for left-sided breast cancer when estimating normal tissue complications in the heart and lung [e-pub ahead of print]. Phys Med Biol 2020 2020. 10.1088/1361-6560/abd230 accessed August 22, 2021.
143. Carabe A, España S, Grassberger C, Paganetti H. Clinical consequences of relative biological effectiveness variations in proton radiotherapy of the prostate, brain and liver. Phys Med Biol 2013;58 2103–2017. [PubMed: 23470339]
144. Tilly N, Johansson J, Isacsson U, et al. The influence of RBE variations in a clinical proton treatment plan for a hypopharynx cancer. Phys Med Biol 2005;50:2765–2777. [PubMed: 15930601]
145. Frese MC, Wilkens JJ, Huber PE, Jensen AD, Oelfke U, Taheri-Kadkhoda Z. Application of constant vs variable relative biological effectiveness in treatment planning of intensity-modulated proton therapy. Int J Radiat Oncol Biol Phys 2011;79:80–88. [PubMed: 20382482]
146. Ödén J, Toma-Dasu I, Witt Nyström P, Traneus E, Dasu A. Spatial correlation of linear energy transfer and relative biological effectiveness with suspected treatment-related toxicities following proton therapy for intracranial tumors. Med Phys 2020;47:342–351. [PubMed: 31705671]
147. Chen Y, Grassberger C, Li J, Hong TS, Paganetti H. Impact of potentially variable RBE in liver proton therapy. Phys Med Biol 2018;63 195001. [PubMed: 30183674]
148. Giantsoudi D, Adams J, MacDonald SM, Paganetti H. Proton treatment techniques for posterior fossa tumors: consequences for linear energy transfer and dose-volume parameters for the brainstem and organs at risk. Int J Radiat Oncol Biol Phys 2017;97:401–410. [PubMed: 27986346]
149. Fjæra LF, Li Z, Ytre-Hauge KS, et al. Linear energy transfer distributions in the brainstem depending on tumour location in intensity-modulated proton therapy of paediatric cancer. Acta Oncol 2017;56:763–768. [PubMed: 28423966]

150. Fjæra LF, Indelicato DJ, Ytre-Hauge KS, et al. Spatial agreement of brainstem dose distributions depending on biological model in proton therapy for pediatric brain tumors. Adv Radiat Oncol 2021;6 100551. [PubMed: 33490724]

151. Giantsoudi D, Seco J, Eaton BR, et al. Evaluating intensity modulated proton therapy relative to passive scattering proton therapy for increased vertebral column sparing in craniospinal irradiation in growing pediatric patients. Int J Radiat Oncol Biol Phys 2017;98:37–46. [PubMed: 28587051]

152. Ytre-Hauge KS, Fjæra LF, Rørvik E, et al. Inter-patient variations in relative biological effectiveness for cranio-spinal irradiation with protons. Sci Rep 2020;10:6212. [PubMed: 32277106]

153. Unkelbach J, Paganetti H. Robust proton treatment planning: Physical and biological optimization. Semin Radiat Oncol 2018;28:88–96. [PubMed: 29735195]

154. Unkelbach J, Botas P, Giantsoudi D, Gorissen BL, Paganetti H. Reoptimization of intensity modulated proton therapy plans based on linear energy transfer. Int J Radiat Oncol Biol Phys 2016;96:1097–1106. [PubMed: 27869082]

155. Fager M, Toma-Dasu I, Kirk M, et al. Linear energy transfer painting with proton therapy: A means of reducing radiation doses with equivalent clinical effectiveness. Int J Radiat Oncol Biol Phys 2015;91:1057–1064. [PubMed: 25832696]

156. Giantsoudi D, Grassberger C, Craft D, Niemierko A, Trofimov A, Paganetti H. LET-guided optimization in IMPT: feasibility study and clinical potential. Int J Radiat Oncol Biol Phys 2013;87:216–222. [PubMed: 23790771]

157. Bassler N, Jäkel O, Søndergaard CS, Petersen JB. Dose- and LET-painting with particle therapy. Acta Oncol 2010;49:1170–1176. [PubMed: 20831510]

158. Joiner M, Kogel AVD. Basic clinical radiobiology. 5th Boca Raton, FL: CRC Press/Taylor & Francis Group; 2018.

159. Fowler JF. Applications to radiobiology and radiotherapy. Int J Radiat Appl Instrum Nucl Tracks Radiat Meas. 1989;16:89–95.

160. Kehwar TS. Analytical approach to estimate normal tissue complication probability using best fit of normal tissue tolerance doses into the NTCP equation of the linear quadratic model. J Cancer Res Ther 2005;1:168–169. [PubMed: 17998649]

161. Bentzen SM. Quantitative Clinical Radiobiology. Acta Oncologica 1993;32:259–275. [PubMed: 8323764]

162. Sheline GE, Wara WM, Smith V. Therapeutic irradiation and brain injury. Int J Radiat Oncol Biol Phys 1980;6:1215–1228. [PubMed: 7007303]

163. Scheenstra AEH, Rossi MMG, Belderbos JSA, Damen EMF, Lebesque JV, Sonke J-J. Alpha/beta ratio for normal lung tissue as estimated from lung cancer patients treated with stereotactic body and conventionally fractionated radiation therapy. Int J Radiat Oncol Biol Phys 2014;88:224–228. [PubMed: 24331668]

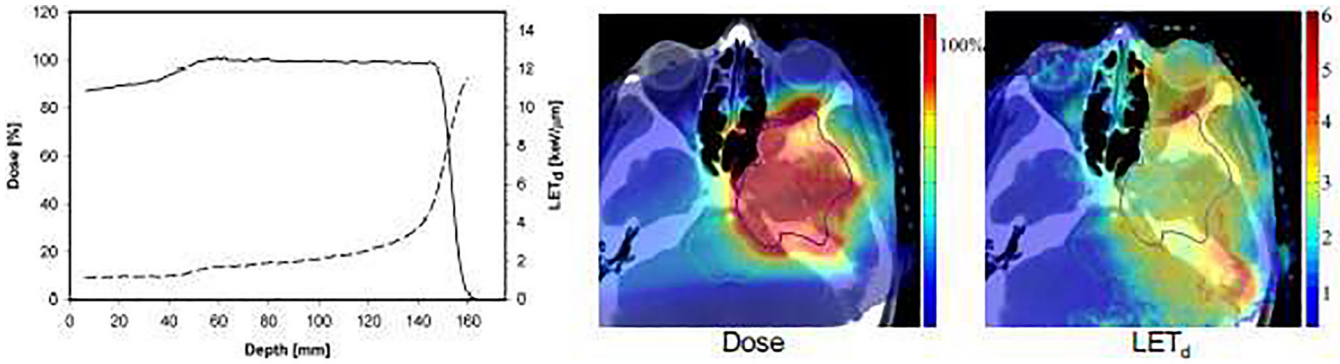

Figure 1:

Left side: Typical ranges of linear energy transfer (dashed line; dose-averaged LET_d) in a spread-out Bragg peak (solid line) in water. Right side: Dose (%) and LET_d (keV/μm) in a chordoma patient based on intensity modulated proton therapy. Figure adapted from [9, 21].

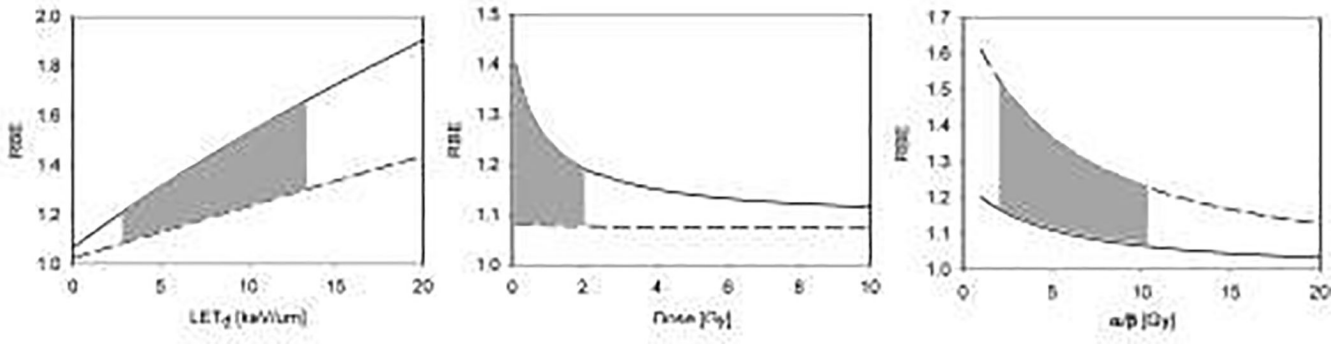

Figure 2:

Proton RBE for clonogenic cell survival as predicted by an empirical model (equation 2) [4]. Left: RBE as a function of LET at 2 Gy (solid $(\alpha/\beta)_x$=2 Gy; dashed $(\alpha/\beta)_x$=10 Gy). The grey area shows the clinically and dosimetrically most relevant region as LET values are typically between 2.5 and 13 keV/μm [21]. Middle: RBE as a function of dose for LET=2.5 keV/μm (solid $(\alpha/\beta)_x$=2 Gy; dashed $(\alpha/\beta)_x$=10 Gy). The grey area shows the clinically most relevant region for a standard 2 Gy fractionation, i.e., doses to organs at risk <2Gy. Right: RBE as a function of $(\alpha/\beta)_x$ for a dose of 2 Gy (solid LET=2 keV/μm; dashed LET=10 keV/μm). The grey area shows the clinically most relevant region of $(\alpha/\beta)_x$=2–10 Gy.

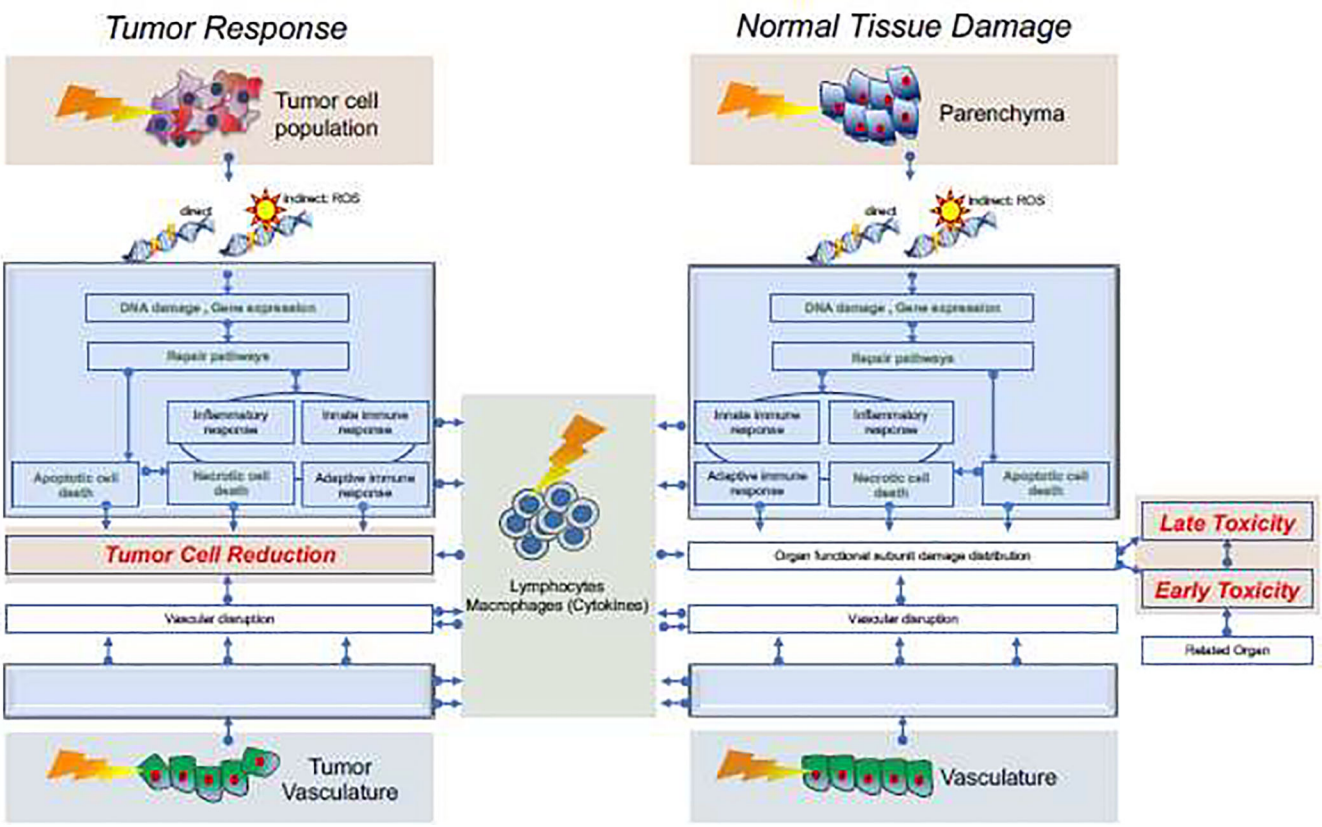

Figure 3:

Schematics of some relevant pathways leading to tumor cell kill and normal tissue toxicities. Starting with direct and indirect DNA damage to the tumor and parenchyma, there are repair pathways that, upon failure, lead to cell kill of tumor cells (left) or damage to functional subunits (right). The text in green indicates pathways related to in vitro cell kill studies. In addition to direct damage to cells, there is radiation-induced damage to vasculature leading to vascular disruption which impacts tumor and normal tissue response. Similarly, adaptive and innate immune response are impacted by radiation. Clinically relevant endpoints are indicated in red. Note that the two empty blue boxes are placeholders for mirrored images of the upper two blue boxes.

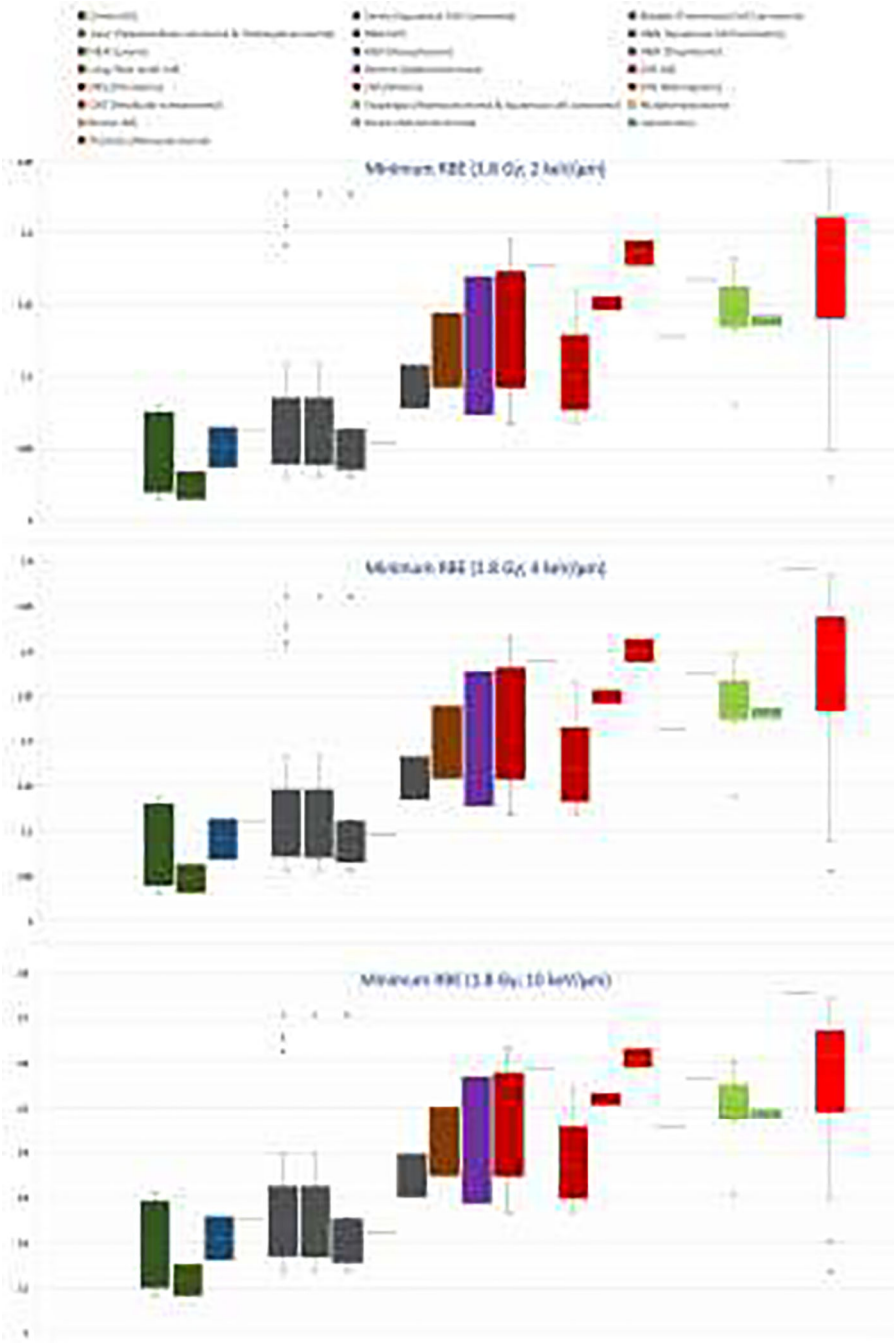

Figure 4:

Proton RBE at 1.8 Gy per fraction based on tumor $(\alpha/\beta)_x$ values extracted from clinical data [64–67] (excluding data with negative values) assuming RBE as a function of $(\alpha/\beta)_x$) as deduced from clonogenic cell survival (equation (2) [4]) and LET estimates [21]. Upper: LET of 2 keV/μm representative for the proximal part of the tumor and likely a minimum conservative RBE; Middle: LET of 4 keV/μm representative for the distal part of the target; Lower: LET of 10 keV/μm as a maximum for the target.

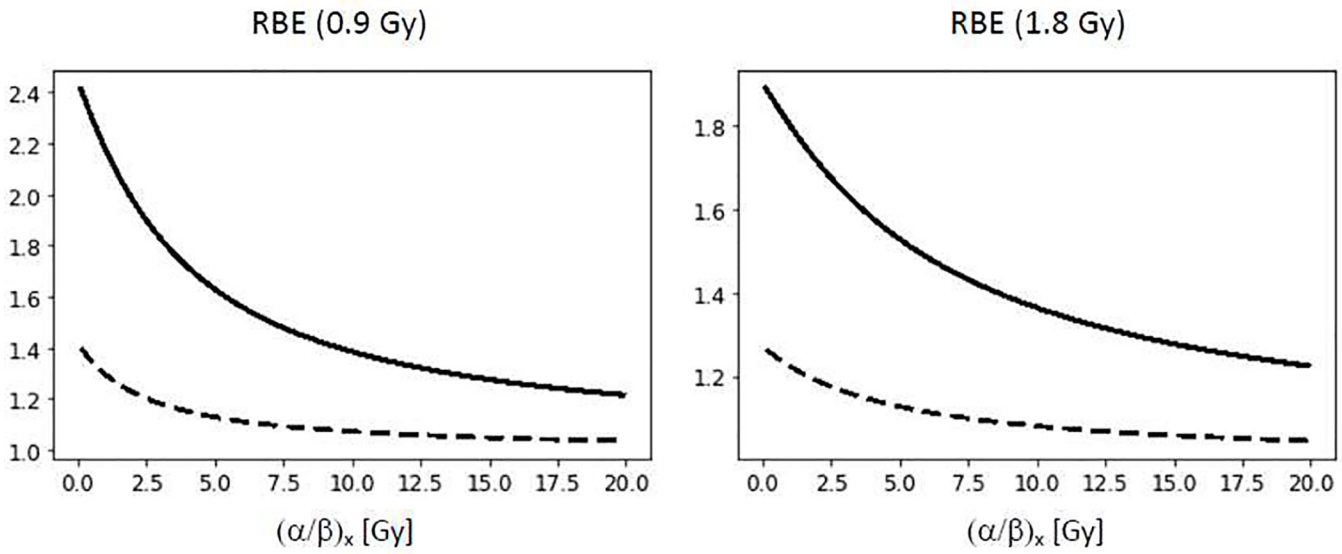

Figure 5:

Proton RBE for clonogenic cell survival as predicted by an empirical model [4]. Left: RBE as a function of $(\alpha/\beta)_x$ at 0.9 Gy (representative of 50% target dose for standard fractionation) for LET=2 keV/μm (dashed) and 10 keV/μm (solid). Right: RBE as a function of $(\alpha/\beta)_x$ at 1.8 Gy for LET=2 keV/μm (dashed) and 10 keV/μm (solid). The two LET values are representative for the entrance region and the distal fall-off of an SOBP field.

Table 1:

Conservative tumor RBE values (Figure 3) in comparison to RBE values from data on clonogenic cell survival in vitro either measured directly or based on $(\alpha/\beta)_x$ and equation (1) (for references see figure 3 and text). As some laboratory experiments use 200–250 kVp X-rays as reference radiation, experimental RBE values were corrected by 1.1–1.15 to relate to 6-MV photons [9]. Also, data were corrected to correspond to ~1.8 Gy per fraction.

	Based on Clinical Data			**Based on in vitro Clonogenic Cell Survival**		
	Range of $(\alpha/\beta)_x$ [Gy]	**Minimum target RBE according to equation (2)**	**Maximum target RBE according to equation (2)**	**Range of $(\alpha/\beta)_x$ [Gy]**	**Minimum RBE reported or according to equation (1)**	**Maximum target RBE reported or according to equation (1)**
Breast	2.2 – 4.6	1.08 – 1.18	1.31 – 1.60		< 0.93	
Breast adenocarcinoma	4 – 4.4	1.14	1.48 – 1.50			
CNS	1.8 – 12.5	1.07 – 1.19	1.27 – 1.63			
CNS chordoma	2.4	1.18	1.59			
CNS glioma	3.1 – 12.5	1.07 – 1.16	1.27 – 1.55	1.83	1.1 – 1.35	1.7 – 1.8
CNS meningioma	3.3 – 3.8	1.15 – 1.16	1.51 – 1.53			
CNS vestibular schwannoma	1.8 – 2.4	1.18 – 1.19	1.59 – 1.63			
H&N	0.9 – 30	1.03 – 1.23	1.14 – 1.71			
H&N squamous cell carcinoma	0.9 – 29.2	1.03 – 1.23	1.14 – 1.71	1.46 – 47.5	0.9 – 1.4	> 2.1
H&N squamous cell carcinoma (larynx)	0 – 29.2	1.03 – 1.23	1.14 – 1.71	1.82 – 7.65	1.2 – 1.4	> 2.1
H&N squamous cell carcinoma (nasopharynx)	16	1.05	1.22			
H&N squamous cell carcinoma (oropharynx)	6.5 – 10.3	1.08 – 1.11	1.30 – 1.40			
H&N salivary gland				0.58 – 10.89	1.0 – 1.1	
GI liver	13.4	1.06	1.46		< 1.15	
GI esophagus	4.9	1.13	1.25		< 1.0 – 1.6	
GI esophagus adenocarcinoma					< 0.6 – 1.0	
GI esophagus squamous cell carcinoma					< 0.7 – 2.3	
GI pancreas adenocarcinoma					0.7 – 2.4	
GU prostate adenocarcinoma	0 – 20	1.03 – 1.24	1.14 – 1.74	5.8	1.0 – 1.85	> 2.0
GU colorectal				3.08 – 69.5	< 1.0	
GU colon					< 1.21	
GU cervix	10 – 52.6	1.01 – 1.08	1.08 – 1.31	6.9 – 7.1	1.07	> 1.28
GU cervix squamous cell carcinoma	26 – 52.6	1.01 – 1.03	1.08 – 1.15			

	Based on Clinical Data			Based on in vitro Clonogenic Cell Survival		
	Range of $(\alpha/\beta)_x$ [Gy]	**Minimum target RBE according to equation (2)**	**Maximum target RBE according to equation (2)**	**Range of $(\alpha/\beta)_x$ [Gy]**	**Minimum RBE reported or according to equation (1)**	**Maximum target RBE reported or according to equation (1)**
GU rectum	2.7 – 11.1	1.07 – 1.17	1.29 – 1.57			
GU bladder	13 – 24	1.04 – 1.06	1.16 – 1.26			
Sarcoma	0.4	1.25	1.75	7.61	1.02	
Lung (Non-small cell)	3.9 – 8.2	1.09 – 1.14	1.35 – 1.50	3.0 – 52.23	0.97 – 1.77	2.3
Pediatric rhabdomyosarcoma	2.8	1.17	1.56			
Pediatric medulloblastoma				4	1.13	

Table 2

Published values for $(\alpha/\beta)_x$ for selected early and late normal tissue endpoints. Shaded rows indicate endpoints with potentially high relative biological effectiveness due to low $(\alpha/\beta)_x$

Tissue endpoints	$(\alpha/\beta)_x$ [Gy]
Capillarics[158]	3
Connective tissue fibrosis[158]	2
Skin nccrosis/fibrosis[159,160]	1.9–2.3
Skin (dermatitis [erythema, desquamation])[66,158]	8.8–12.3
Skin desquamation[66]	18–35
Skin telangiectasis[66,159]	3.9–5.7
Ncrve (brachial plexopathy)[160,161]	2; < 5.3
Nerve (cauda equina)[160]	2–3
Breast (atrophy, fibrosis)[158]	2–3
Heart (peri card i ti s)[158,160]	2–3
Chiasm (loss of visión)[158,160]	2–3
Optic nerve (ncuropathy)[158]	2
Larynx (chronic edema, fibrosis)[158,160]	2–4
Larynx: cartilage necrosis and edema[66,160]	3.4–4.4
Salivary glands (xerostomia)[158]	3
Oral museositis[158]	10
Hairloss[158]	7
Oropharynx: late effects[66]	4.5
Brain/brainstcm necrosis[160,162]	2.1
Spinal cord myelopathy/necrosis[66,160]	2; <3.3
Livcr fibrosis[158]	1
Liver failure[160]	1.5
Esophagus (stricturc/pcrforation)[160]	3
Kidney ncphritis/ncphropathy[158,160]	2–3.5
Stomach (ulccration/pcrforation)[158,160]	4; 7–10
Colon (obstruction/ulccration/pcrforation)[160]	3.1–5
Rcctum (stcnosis/proctitis/necrosis)[160]	3.9
Rectum (chronic inflammation, ulcer)[160]	5
Small intestinc (obstruction/pcrforation)[160]	6–8.3
Bowel (stricture/perforation)[66]	2.2–8
Bladder[160]	3.4–6
Urinary bladder cystitis[158]	10
Ccrvical/thoracic/lumbar myelopathy[158]	2
Lung perfusion[163]	1.3
Lung fibrosis[158,159]	3–3.6; 4
Lung pneumonitis[66,159,160]	< 3.8; 4.4–6.9

Tissue endpoints	$(\alpha/\beta)_x$ [Gy]
Lung pneumonitis (early)[66,158]	> 8.8; 5
Rib fractures[159,160]	1.8–2.5
Bone (osteoradionecrosis)[158]	60